jmr&t Journal of Materials Research and Technology

www.jmrt.com.br

Original article

Compatibility of 9Cr–1Mo steel exposed to thermally convective Pb–17Li

Poulami Chakraborty[a,*], *Pankaj Kumar Pradhan*[b], *Ram Krishen Fotedar*[a], *Nagaiyar Krishnamurthy*[a]

[a] *Fusion Reactor Materials Section, Bhabha Atomic Research Centre, Mumbai, India*

[b] *Materials Processing Division, Bhabha Atomic Research Centre, Mumbai, India*

ARTICLE INFO

Article history:
Received 3 October 2012
Accepted 16 April 2013
Available online 29 July 2013

Keywords:
9Cr–1Mo
Pb–17Li
SEM-EDS
EPMA

ABSTRACT

Corrosion behavior of 9Cr–1Mo steel (P91) with flowing Pb–17Li has been studied in a thermal convection loop at a thermal gradient of 100 K between the hot and cold legs and a flow velocity of 6 cm/s. After 1000 h of operation, samples of P91 from both hot and cold legs were analyzed with the help of weight change measurements, Scanning Electron Microscopy coupled with Energy Dispersive Spectrometry (SEM-EDS) and Electron Probe Micro Analysis (EPMA). The results showed preferential dissolution of constituent elements like Fe and Cr from the hot leg samples leading to weight loss, though penetration of Pb–17Li into the inner matrix was not observed. No corrosion was found in the cold leg and the sample surface was found to contain deposits of the elements dissolved from hot leg.

1. Introduction

One of the key challenges in the march toward demonstration of an engineered nuclear fusion reactor concerns the compatibility of materials with the potential coolants. With an objective to provide in-house breeding of tritium, lead–17 at.% lithium eutectic (Pb–17Li) has been proposed by many researchers as the coolant, breeder and neutron multiplier for fusion systems. This material provides effective tritium breeding and is safer, relative to molten lithium, under accident conditions since it is less reactive with air and water [1]. However, Pb–17Li has been found to be more corrosive toward structural materials than pure lithium and the corrosion rate is affected by various factors like temperature, flow velocity, etc [1,2]. Along with that, the accumulation of corrosion products in the cooler areas is expected to cause flow restrictions that can increase pumping power requirements and decrease heat transport. In this regard, different classes of structural materials have been investigated for their corrosion compatibility with Pb–17Li in static and dynamic systems [3–6]. The corrosion mechanism is generally governed by solubility driven mass transfer [7]. It was found that austenitic steels have a poor resistance to Pb–17Li because of the high solubility of nickel [7,8]. Presently, ferritic martensitic steels have come up as better candidates for fusion reactor applications due to their higher irradiation stability and are expected to have better compatibility due to their very low nickel content

* *Corresponding author.*
E-mail: myworld.pc@gmail.com (P. Chakraborty).

2238-7854 http://dx.doi.org/10.1016/j.jmrt.2013.04.001

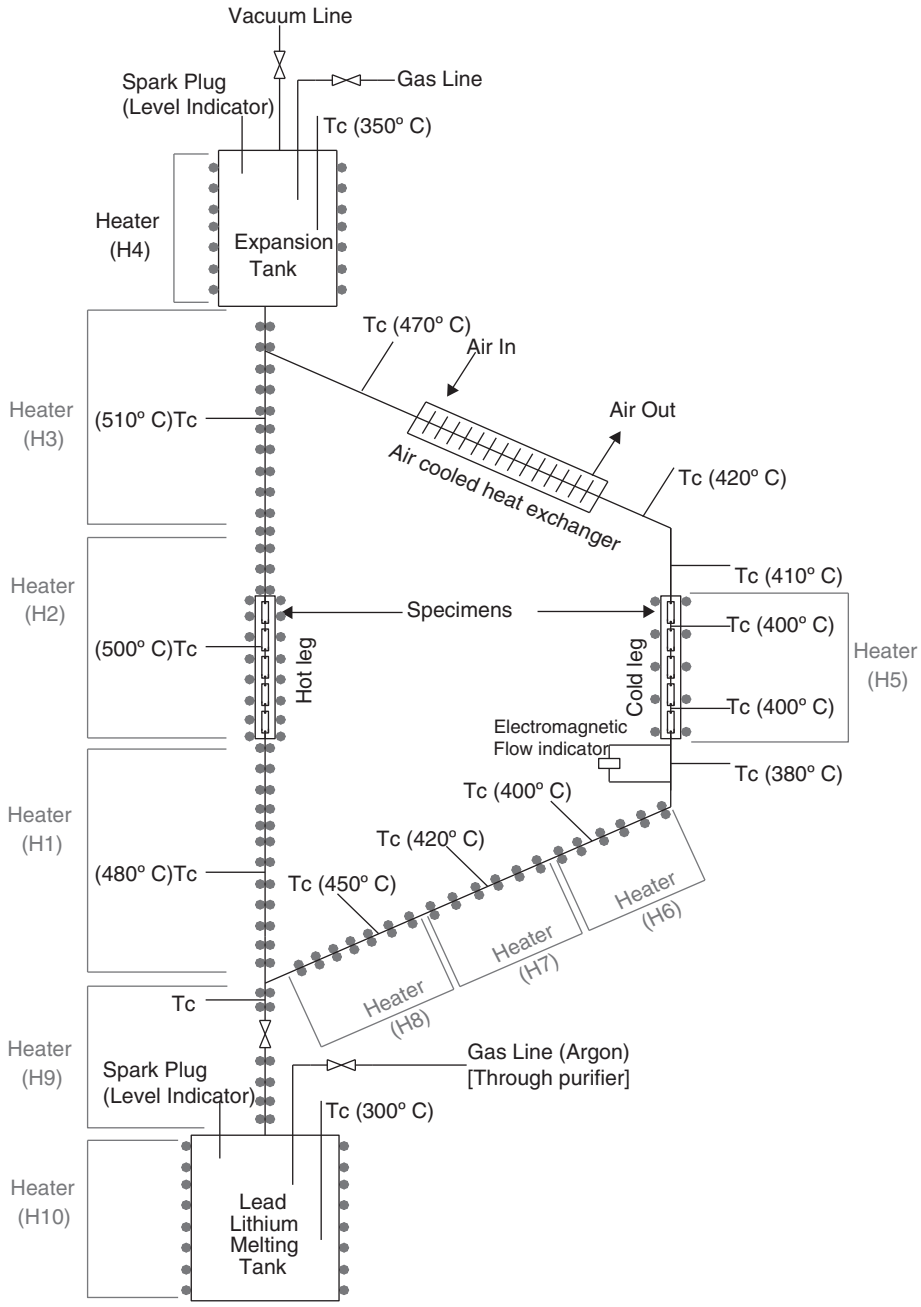

Fig. 1 – Schematic drawing of the thermal convection loop.

[9,10]. Modified 9Cr–1Mo steel (P91) is such a steel developed in the 1970s as part of a program for developing advanced creep resistant alloys for fast breeder power reactor programs [10–12]. The present paper discusses the results obtained from a 1000 h experiment to study the corrosion behavior of P91 steel in a thermally convective flow of Pb–17Li [4]. Samples have been exposed both at the hot and cold legs such that dissolution and deposition data could be presented together.

2. Experimental

The experiment was conducted in a 0.8 L capacity thermal convection loop as shown in Fig. 1. For the present study, modified 9Cr–1Mo (P91) coupons in normalized and tempered condition and having dimensions of 10 mm × 35 mm × 2 mm were placed in the loop. Five such samples each were placed in the hot and cold legs at locations indicated in Fig. 1. The chemical composition of P91 material taken from the unexposed coupons is given in Table 1. The entire loop was fabricated from a combination of SS316L and P91 pipes having 12 mm internal diameter and 2 mm wall thickness. P91 material was used for fabricating the hot leg region of the loop whereas SS316L was used for the rest. Kanthal heaters (H) of different capacities along with K type thermocouples (T_c) were wrapped on the pipe as indicated in Fig. 1. Spark plugs acted as conduction probes for level indicators in the melt tank and expansion tank. Pb–17Li chunks were placed in the

Table 1 – Chemical composition of the P91 steel.

Elements	C	Cr	Mo	Mn	Ni	V	Nb	Fe
wt.%	0.006	9.12	1.09	0.39	0.14	0.25	0.14	Balance

melt tank and a positive cover gas pressure of purified argon was maintained over the entire loop. Expansion tank allows accommodating the volumetric changes in the liquid eutectic during heating or cooling operations and other temperature fluctuations. Initially, the temperature of the entire loop along with the melt tank was raised and maintained at 573 K. Filling operation of the entire loop was carried out by gas pressurization method till desired level was achieved as indicated by expansion tank level sensor. After filling of the loop, the power input to different heaters was adjusted in such a way that the samples at hot leg experienced a uniform temperature of 773 K (500 °C) whereas those at the cold leg were maintained at 673 K (400 °C). The air cooled heat exchanger facilitated cooling of the liquid eutectic to desired temperature before entering the cold leg. A flow velocity of 6 cm/s for the molten eutectic was achieved through a temperature gradient of 100 K as measured by the electromagnetic flow meter attached at the cold leg.

After 1000 h of operation, molten Pb–17Li was drained back into the melt tank and all the P91 samples were taken out under argon atmosphere. A few of the samples from both the legs were cleaned off the adhering Pb–17Li by repeatedly exposing to a solution of acetic acid, ethyl alcohol and hydrogen peroxide mixed in the ratio of 1:1:1. Both these cleaned and the rest un-cleaned samples were used for further characterization.

The corrosion rate of P91 steel in thermally convective Pb–17Li was calculated as a function of time using weight loss measurements. The corroded surfaces were observed and analyzed for environmentally induced compositional changes. Microstructural and compositional data were obtained from Scanning Electron Microscopy coupled with Energy Dispersive Spectrometry (SEM-EDS) and Electron Probe Micro Analysis (EPMA). For the above characterization purposes, the samples were etched in Picral (picric acid:ethyl alcohol = 1:1). The lead–lithium eutectic after exposure was analyzed by Inductively Coupled Plasma – Atomic Emission Spectroscopy (ICP-AES).

3. Results

Weight loss data for hot leg samples indicated sufficient dissolution from P91 at 773 K. As observed from Table 2, the dissolution rates were higher at the upstream side probably due to greater temperature stabilization in this zone. On the other hand, an increase in weight was observed for P91 samples placed at 673 K in the cold leg. As indicated in Table 3, the deposition of corrosion product was higher downstream in the cold leg. This was possibly due to the effect of gravity on the deposition process. For a period of 1000 h, an average dissolution rate 17 μg/cm^2 h and an average deposition rate of 1.2 μg/cm^2 h was obtained.

Table 2 – Dissolution rate for hot leg samples at 773 K.

	Initial weight (g)	Final weight (g)	Loss (g)	Dissolution rate (μg/cm h)
Upstream	4.2209	4.0150	0.2059	20.3
Downstream	4.5219	4.3745	0.1474	14.5

Table 3 – Deposition rate for cold leg samples at 673 K.

	Initial weight (g)	Final weight (g)	Gain (g)	Deposition rate (μg/cm h)
Upstream	4.3091	4.3205	0.0114	1.12
Downstream	4.1651	4.1651	0.0139	1.37

Table 4 – Composition of lead–lithium eutectic from hot and cold leg.

	Cr	Fe	Mo
Hot leg	58	158	83
Cold leg	7	62	27

After draining the liquid metal into the melt tank, adherent Pb–17Li from hot and cold legs were subjected to chemical analysis and the results are reported in Table 4. The idea was to find the difference in dissolved species concentration in the liquid metal at higher and lower temperature. The results indicated a much lower content of Cr, Mo and Fe in the cold leg sample than in the hot leg.

The P91 samples were subjected to structural and compositional analysis before and after cleaning of the adherent layer of Pb–17Li. Fig. 2a shows a prominent whitish layer of lead–lithium eutectic on the un-cleaned sample exposed at 773 K in the hot leg. It could be noted from the SEM image at Fig. 2b that this layer is finely divided into two sublayers. The composition of the two layers as obtained from EDS is reported in Table 5. The outer layer indicated the presence of 24% oxygen whereas the inner layer contained small amount of chromium and iron along with 14% oxygen, indicating that metallic species had dissolved into the adjacent liquid metal during the loop operation. Lithium could not be detected due to limitation in EDS. After cleaning of the hot leg sample, a thin

Table 5 – Composition of outer and inner layer of lead–lithium alloy on P91 specimen at 773 K.

Element	Outer layer of Pb–17Li	Inner layer of Pb–17Li
Lead	74.83	81.30
Oxygen	24.56	14.56
Iron	0.61	2.44
Chromium	–	1.19
Nickel	–	0.61

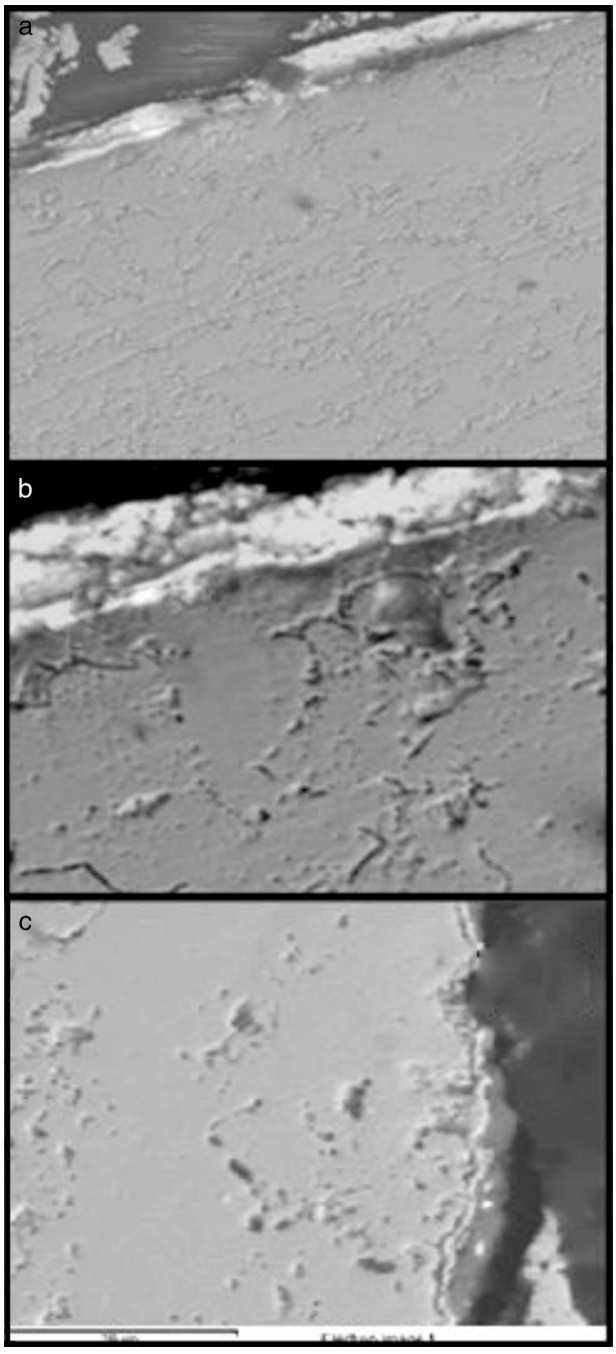

Fig. 2 – Cross section of P91 samples placed in the hot leg at 773 K; (a) uncleaned sample, (b) uncleaned sample with double layer of lead–lithium deposit and (c) cleaned sample.

corroded layer was observed along the boundary as shown in Fig. 2c. When elemental line scans were taken across this layer, both Fe and Cr were found to drop down from their matrix values near the interface as shown in Fig. 3.

Further analysis of the corroded surface was carried out on hot leg samples using EPMA. Fig. 4 shows the back scattered image of the P91 sample from hot leg of buoyancy loop. Composition scans of iron, chromium and lead, as depicted in Fig. 5a–c respectively, were taken along the red line in Fig. 4. It was observed that Fe and Cr got depleted from a very shallow

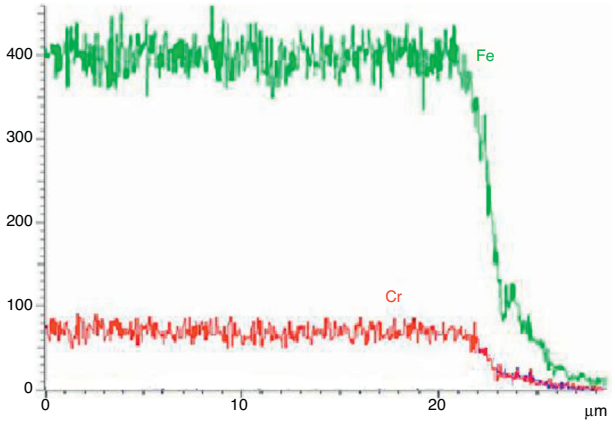

Fig. 3 – Profile of Fe and Cr across the P91 surface facing lead–lithium at 773 K.

Table 6 – Average composition of deposits at 673 K from EDS analysis.

Element	Deposit
Iron	33.34 ± 1.2
Chromium	65.69 ± 1.9
Nickel	0.98 ± 0.08

surface layer. The depth of this layer was not more than 4 μm. On the other hand, no penetration of lead into the matrix along this surface layer was observed.

Analysis of the un-cleaned sample kept at 673 K in the cold leg indicated a much thicker deposit of Pb–17Li as shown in Fig. 6a. EDS at the interface gave no evidence of dissolution since the composition remained similar to matrix composition. Cleaning of the sample revealed smaller deposits scattered over the surface as could be observed from the SEM image in Fig. 6b. From the average composition taken over a

Fig. 4 – BSE image of hot leg P91 sample. Straight line across the boundary represents the direction of EPMA scans.

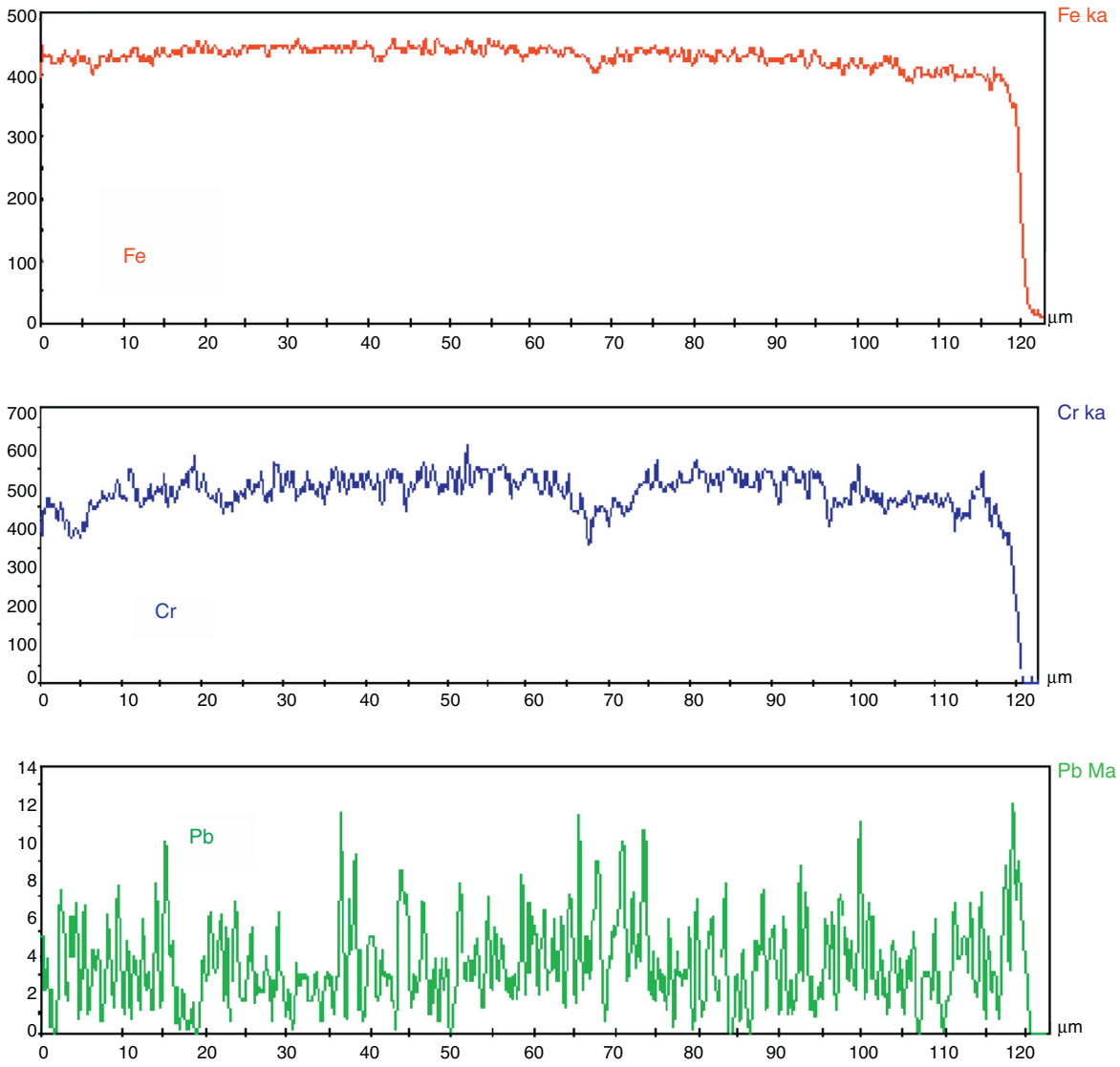

Fig. 5 – EPMA profiles for iron, chromium and lead across the exposed P91 surface at 773 K.

number of deposits (Table 6), it could be observed that they were significantly richer in chromium.

4. Discussion

It was observed that the corrosion rate of 17 μg/cm^2 h for P91 steel was lesser than that of austenitic steels under similar conditions (i.e. 27 μg/cm h) [7]. The obvious reason for this is the presence of negligible quantity of nickel in ferritic–martensitic steels like 9Cr–1Mo. In this context, it has been already established that nickel has the highest solubility in Pb–17Li [13] and constitutes the major portion of the dissolved species in case of austenitic stainless steel. Deposition of dissolved species in the cold leg was due to lowering of solubility limit in lead–lithium eutectic at lower temperature (673 K) thus leading to weight gain [14]. Since deposition was much lesser than dissolution, it was evident that large amounts of dissolved products must have remained in the liquid itself. The same was confirmed from the chemical analysis of the lead–lithium eutectic.

Corrosion of modified 9Cr–1Mo steel in Pb–17Li is initiated by dissolution of the oxide scale present on its surface. It has been confirmed by Konys et al. that during vacuum heat treatment, a two layer oxide scale develops on P91 surface, containing an inner layer of (Fe, Cr)$_2$O$_3$ and an outer layer of MnCr$_2$O$_4$ [15]. They also established that corrosion of steel matrix begins only after dissolution of these oxides in the liquid alloy. Thus, interaction of Pb–17Li with this scale could result in oxidation of lithium and presence of lead-oxide in the layer adherent to the P91 surface. The inner layer of this oxide scale containing metallic species like iron and chromium is expected to contain the reaction products of the above interaction. On cleaning the P91 samples, the non-uniformly corroded surface was observed in Fig. 2c. This predicts that dissolution of the oxide scale had occurred non-uniformly thus exposing fresh P91 surface to the Pb–17Li alloy. Similar observations have been also made by Konys et al. [15] Afterwards, leaching of soluble alloying elements like Fe and

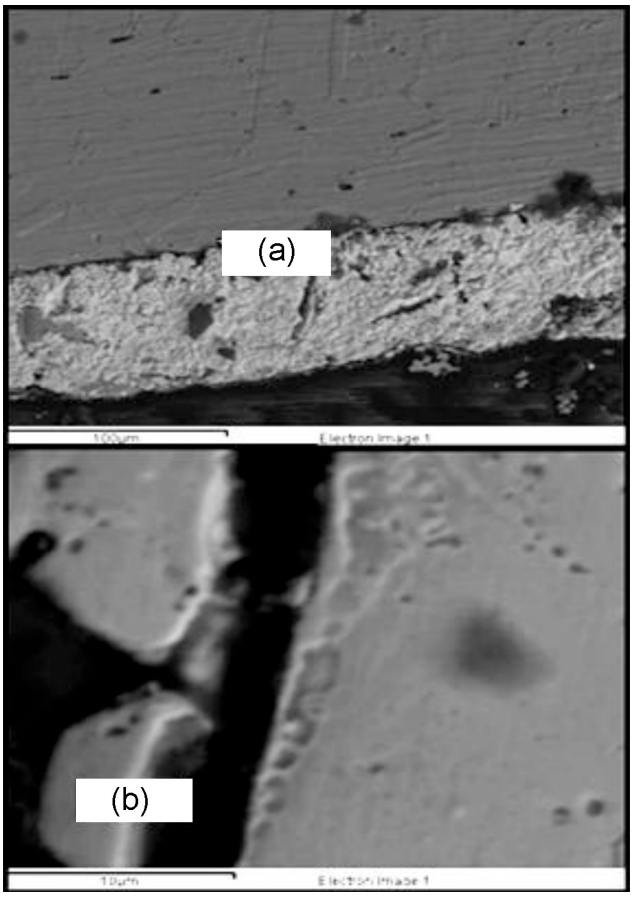

Fig. 6 – P91 sample placed in the cold leg at 673 K (a) uncleaned sample, (b) cleaned sample showing deposits.

Cr, from the steel surface into the Pb–17Li had started thereby causing a weight loss as indicated in Table 1. This led to the formation of a 4 μm deep depleted layer on the surface as observed in EPMA scans.

From the analysis of P91 samples kept in the cold leg, it was clear that corrosion by Pb–17Li does not place at 673 K. The dissolved species in the hot leg were transported to the cold leg through the liquid eutectic and were precipitated out on the cold leg sample surface. This fact is confirmed from the chemical analysis of Pb–17Li which has shown higher quantities of metallic species like Fe, Cr and Mo present in the hot leg. On an average, such deposits were found to be chromium rich and this may be due to a significantly lesser solubility of Cr in Pb–17Li at 673 K [16]. This led to higher precipitation of chromium as compared to the other elements which can be additionally confirmed from the adherent Pb–17Li composition which shows a significant reduction of Cr content at 673 K.

5. Conclusions

Modified 9Cr–1Mo steel (P91) samples were exposed to Pb–17Li at 773 K and 673 K in the hot and cold leg of a thermal convection loop, respectively. After 1000 h, a corrosion rate of 17 $\mu g/cm^2$ h for P91 samples kept at 773 K and a deposition rate of 1.2 $\mu g/cm^2$ h on P91 samples at 673 K were obtained. Analysis of the test results has revealed that corrosion of P91 initiates by dissolution of the oxide scale present on its surface. This dissolution is non-uniform and thus creates a non-uniformly exposed P91 surface from which corrosion proceeds mainly by the dissolution of major alloying elements like Cr and Fe into Pb–17Li. In the present condition dissolution takes place from a depth of 4 μm from the surface and no penetration of Pb–17Li occur into the inner matrix of P91. The dissolved species get deposited in the colder regions of the loops. Due to the lower solubility of Cr in Pb–17Li at 673 K, these deposits are found to be richer in chromium.

Conflicts of interest

The authors declare no conflicts of interest.

Acknowledgements

We would like to thank Mr. Bhaskar Paul, M.P.D., B.A.R.C., for carrying out the SEM-EDS analysis and Mr. A. Laik, M.S.D., B.A.R.C., for helping in the E.P.M.A. study.

REFERENCES

[1] Atanov A, Chepovski A, Gromov V, Kalinin G, Markov V, Rybin V, et al. Properties and behaviour of 83Pb–17Li eutectic. Fusion Eng Des 1991;14:213–8.
[2] Malang S, Mattas R. Comparison of lithium and the eutectic lead–lithium alloy, two candidate liquid metal breeder materials for self-cooled blankets. Fusion Eng Des 1995;27:399–406.
[3] Tortorelli PF, DeVan JH. Surface analysis of ferrous alloys exposed to static Pb–17 at.% Li. J Nucl Mater 1984;123:1264.
[4] Tortorelli PF, DeVan JH. Corrosion of ferrous alloys exposed to thermally convective Pb–17 at% Li. J Nucl Mater 1986;141–143:592–8.
[5] Chopra O, Smith D. Corrosion of ferrous alloys in eutectic lead–lithium environment. J Nucl Mater 1984;123:1219–24.
[6] Chakraborty P, Kumar S, Fotedar RK, Suri AK.Proceedings of the 3rd international symposium on materials chemistry. 2010. p. 73.
[7] Tortorelli PF. Dissolution kinetics of steels exposed in lead–lithium and lithium environments. J Nucl Mater 1992;191–194:965–9.
[8] Simon N, Terlain A, Flament T. The compatibility of austenitic materials with liquid Pb–17Li. Corros Sci 2001;43:1041–52.
[9] Klueh RL, Nelson AT. Ferritic/martensitic steels for next-generation reactors. J Nucl Mater 2007;371:37–52.
[10] Saroja S, Dasgupta A, Divakar R, Raju S, Mohandas E, Vijayalakshmi M, et al. Development and characterization of advanced 9Cr ferritic/martensitic steels for fission and fusion reactors. J Nucl Mater 2011;409:131–9.
[11] Hsu C-Y, Lechtenberg TA. Microstructure and mechanical properties of unirradiated low activation Ferritic steel. J Nucl Mater 1986;141–143:1107–12.
[12] Zeman A, Debarberis L, Kočík J, Slugeň V, Keilová E. Microstructural analysis of candidate steels pre-selected for new advanced reactor systems. J Nucl Mater 2007;362:259–67.
[13] Borgstedt HU, Feuerstein H. The solubility of metals in Pb–17Li liquid alloy. J Nucl Mater 1992;191–194:988–91.

[14] Lyublinski IE, Evtikhin VA, Pankratov VYu, Krasin VP. Numerical and experimental determination of metallic solubilities in liquid lithium, lithium-containing nonmetallic impurities, lead and lead–lithium eutectic. J Nucl Mater 1995;224:288–92.
[15] Glasbrenner H, Konys J, Röhrig HD, Stein-Fechner K, Voss Z. Corrosion of ferritic–martensitic steels in the eutectic Pb–17Li. J Nucl Mater 2000;283–287:1332–5.
[16] Tortorelli PF. Deposition behavior of ferrous alloys in molten lead–lithium. Fusion Eng Des 1991;14:335–45.